

## Bloch Oscillations in an Array of Curved Optical Waveguides

G. Lenz

*Lucent Technologies, Bell Labs, 700 Mountain Avenue, Murray Hill, New Jersey 07974-0636*

I. Talanina and C. Martijn de Sterke

*School of Physics, University of Sydney, NSW 2006, Australia*

(Received 11 February 1999)

We propose to use periodically spaced, curved optical waveguides for observation of optical Bloch oscillations. The refractive index distribution in this system is equivalent to the sum of a periodic term resulting from the equal spacing of the waveguides and a linear ramp, created by the curvature. We demonstrate numerically that light propagation in this geometry exhibits spatial Bloch oscillations with the period depending on the radius of the curvature and the wavelength.

PACS numbers: 42.25.Bs, 42.82.Et, 78.90.+t

In 1928 Bloch predicted that a charge carrier in an ideal crystal placed in a uniform electric field exhibits periodic oscillations [“Bloch oscillations” (BO)]: The carrier is accelerated by the electric field until its momentum satisfies the Bragg condition associated with the periodic potential and is reflected. The carrier is then decelerated by the field until it stops, completing one Bloch cycle [1]. This periodic motion is intimately related to a Wannier-Stark ladder (WSL) energy spectrum, the ladder of equally spaced states with energy spacing given by the potential drop per period [2].

There are two main obstacles to observing BO in solids: (i) The band structure of crystals may be complex and many types of electronic carriers, such as conduction electrons and heavy and light holes, may be involved; (ii) even for fields approaching breakdown, the mean collision-free path of a carrier is smaller than one Bloch period, which is inversely proportional to the period of the potential [3–5]. Only when using high-quality semiconductor superlattices with much larger periodicities than bulk crystals did the observation of BO become feasible, finally to be reported in time-resolved four-wave mixing experiments [6] and measurement of terahertz radiation from the superlattice BO [7]. However, many-body effects can be avoided and the original simplicity of Bloch’s model can be preserved if one exploits neutral species, such as atoms or photons, to observe BO and WSL. Using atoms moving in an accelerating optical lattice created by two interfering laser beams, the observations of atomic WSL and BO were reported recently [8–10].

Two different approaches to create optical WSLs have previously been discussed. It was demonstrated recently that a WSL can be observed in a linearly chirped moiré grating written in the core of an optical fiber [11]. However, in that geometry BO cannot be detected directly. It was also suggested that a WSL may be observed in a dielectric with a refractive index profile that is the sum of a periodic and a linear term [12,13]:

$$n(y + Md) = n(y) + \alpha Md, \quad (1)$$

where  $n(y)$  is a periodic function in the transverse direction  $y$ , and  $\alpha Md$  is a linear ramp which mimics the effect of a uniform electric field ( $d$  is a period discussed below,  $M$  is an integer,  $\alpha$  is a ramp parameter). While the requirement for the periodic potential is easily satisfied using an array of strongly coupled waveguides, imposing a linear variation in the index profile is more challenging. Gradually changing the composition in the transverse direction is very difficult. The other option is imposing a linear change in “effective” index by linearly varying the thickness of the guiding layer. Achieving this uniformly is also difficult and the range of index slopes is limited. Because of these technical difficulties, the associated experiments have not been carried out. We note that, in Ref. [14], a scheme is proposed where the linear ramp is achieved using the electro-optic effect.

In this Letter, we propose a simple and practical optical structure that can demonstrate *optical* Bloch oscillations (OBO). The structure consists of an array of periodically spaced, *curved* optical waveguides. The curvature plays a central role here, effectively leading to a linear ramp in the refractive index distribution. This ramp is superimposed on the periodic index distribution due to the equal spacing of the guides, as required by Eq. (1). Waveguide geometries require light propagation at an oblique angle to the waveguides [12,13]; as a result, OBO occur in *spatial* domain, in contrast to the solid state case where BO occur in time [5]. The Bragg reflection on the high-index side of the structure and the total internal reflection (TIR) on the low-index side trap the light in the transverse direction resulting in spatial oscillations of the path of light along the waveguides (see Fig. 1). The relation of these oscillations to the electronic BO is similar to the relation between the (spatial) oscillations in intensity when light propagates through two coupled waveguides, and the (temporal) quantum beats of electrons in two coupled quantum wells [15].

The advantages to observing BO in a curved waveguide array are as follows: (i) There is only one type of “carrier”—photons, and essentially this is a single band

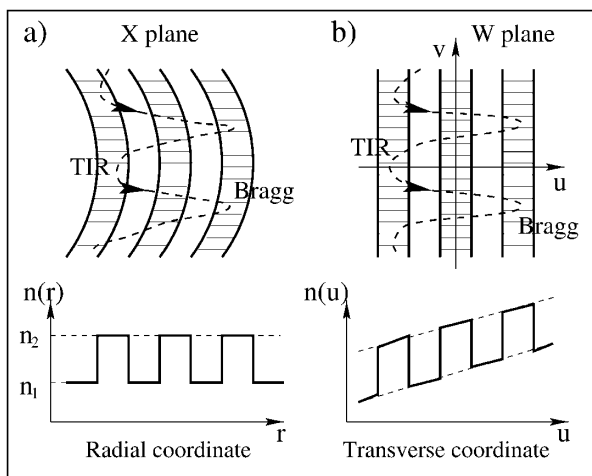


FIG. 1. Top: Schematic of (a) a curved waveguide array and (b) its conformal transformation. The dashed arrows illustrate the light confinement mechanisms—Bragg reflection on one side of the structure and TIR on another side. Bottom: (a) Refractive index in the curved array, and (b) the transformed refractive index. The refractive indices of the guides and the surrounding material are  $n_2$  and  $n_1$ , respectively.

structure. (ii) There are no other excitations, such as phonons, and no carrier-carrier collisions that lead to dephasing and ultimately the destruction of BO. (iii) Fabrication of a curved waveguide array is not more difficult than any standard photonic circuit. The linear potential is controlled by changing the radii which can be very accurately defined. (iv) The OBO can be tuned by varying the wavelength. Here we present an analytical background for OBO in curved waveguide arrays, perform numerical simulations showing OBO along the curves and the corresponding WSL spectrum, and finally address some of the experimental issues associated with observing OBO.

To analyze light propagation in curved waveguides, we use the approach of Heiblum *et al.* [16], based on conformal transformations. To illustrate this method, we consider a coordinate system  $u, v$  which is defined with respect to the original coordinates  $y$  and  $z$  by  $W = u + iv = f(X) = f(y + iz)$ . With the help of the Cauchy-Riemann relations ( $\partial u/\partial y = \partial v/\partial z$ ,  $\partial u/\partial z = -\partial v/\partial y$ ), the two-dimensional scalar wave equation for the envelope function of the light field,  $E(u, v)$ , is expressed as

$$\left[ \nabla_{u,v}^2 + \left| \frac{dX}{dW} \right|^2 k_0^2 n_{\text{eff}}^2(u, v) \right] E(u, v) = 0, \quad (2)$$

where  $k_0$  is the wave number of the light in vacuum,  $n_{\text{eff}}$  is the effective index, and  $\nabla_{u,v}^2 = (\partial^2/\partial u^2) + (\partial^2/\partial v^2)$ .

As shown in Ref. [16], a logarithmic conformal transformation,

$$W = R \ln(X/R), \quad (3)$$

for which

$$\left| \frac{dX}{dW} \right| = \exp(u/R), \quad (4)$$

where  $R$  is a radius of the curvature, converts curved boundaries in the  $X$  plane [see Fig. 1(a)] into straight ones in the  $W$  plane [see Fig. 1(b)]. The transformed refractive index in this equivalent structure is a product of  $\exp(u/R)$  and the refractive index in the appropriate region of the curved guide. For a typical waveguide array, the coordinate  $u$  varies on a micrometer scale, whereas  $R$  varies on a millimeter scale. Thus, the difference between  $\exp(u/R)$  and its Taylor expansion [ $1 + (u/R)$ ] is virtually indistinguishable. Therefore, the ramp in the refractive index distribution can be approximated as linear with the ramp parameter  $\alpha = n_{\text{eff}}/R$ , making this geometry suitable for observation of OBO.

Following the argument in Ref. [13], we obtain a rough estimate for the transverse localization length of the OBO,  $L$ , using the analogy between the behavior of waveguide modes and plane waves with wave vector components  $k_u$  and  $k_v$ . Equation (2) requires that

$$k_u^2 + k_v^2 = n_{\text{eff}}^2 [1 + (u/R)]^2 k_0^2, \quad (5)$$

where we neglect the rapidly varying periodic component of the refractive index for simplicity. Because  $n_{\text{eff}}$  does not depend on  $v$ ,  $k_v$  must be a conserved quantity. The other component,  $k_u$ , is confined by two limiting values:  $k_u = 0$  at  $u = u_1$  (TIR) and  $k_u = \pi/d$  at  $u = u_2$  (Bragg reflection). Substitution of these values into Eq. (5) and taking into account the conservation of  $k_v$  leads to

$$n_{\text{eff}}^2 [1 + (u_1/R)]^2 k_0^2 = n_{\text{eff}}^2 [1 + (u_2/R)]^2 k_0^2 - (\pi/d)^2. \quad (6)$$

Neglecting small terms  $O(\alpha^2 u^2)$  and defining the transverse localization length  $L = u_2 - u_1$ , we obtain

$$L = \left( \frac{\lambda}{2d} \right)^2 \frac{R}{2n_{\text{eff}}^2}, \quad (7)$$

where  $\lambda$  is the wavelength, and  $d$  is a spacing between the waveguides (the period). Equation (7) is valid in the limit when the light is weakly bound to the guides (an optical analog of the nearly free electron model), and, in fact, it gives an upper limit for  $L$ .

The spatial period of the OBO,  $l$ , is derived following the same procedure as for the electronic WSL [5]:

$$l = \frac{\lambda R}{dn_{\text{eff}}}. \quad (8)$$

As seen from Eqs. (7) and (8), both the transverse width of OBO and the period depend linearly on  $R$ . This is similar to the solid state case where the temporal period and the width of the BO depend on the electric field. The temporal period, for example, equals  $h/(eEd)$  [5]. In our case, the equivalent spatial period (8) has an additional

wavelength dependence which has no analogy in the electronic BO and provides an extra degree of freedom allowing us to tune the OBO.

In numerical simulations, we model light propagation in an array of curved  $\text{SiO}_2$ -based waveguides with the following structural and material parameters: The period is  $d = 6 \mu\text{m}$ , the guides' width is  $w = 2.5 \mu\text{m}$ ,  $n_1 = 1.45$ , and  $n_2 = 1.4594$  ( $n_{\text{eff}} = 1.455$ ). For the chosen parameters, an individual waveguide is single moded. By properly exciting this curved array at one end, we launch a superposition of WSL eigenmodes (which correspond to the WSL eigenstates in the electronic case). As an input in the simulations, we launch a Gaussian field distribution with  $\lambda = 1.5 \mu\text{m}$  (unless specified otherwise). The input is centered at the middle of one of the waveguides (the "central" guide). The number of waveguides in the array,  $N$ , is more than 70, so the periodic structure can be considered as infinite. Note that the similar results are obtained for more realistic arrays ( $N$  less than 20).

We solve Eq. (2) using a beam propagation method [17] and compute the intensity of the light field,  $I(u, v) = |E(u, v)|^2$ . Figure 2 shows the light trajectories in an array with  $R = 6 \text{ mm}$  in the  $X$  plane for a propagation angle of  $90^\circ$  corresponding to a propagation length of about 9 mm. As a result of the Wannier-Stark localization, the light is trapped within a narrow region of the array which has a transverse size of about five waveguides. The observed oscillations in the light trajectories are OBO.

The physical effect of curvature in our model is equivalent to one of uniform electric field in the electronic BO. Namely, a decrease in  $R$  leads to a steeper ramp (or stronger electric field in the electronic case) and enhances the light confinement. Indeed, this can be seen from Figs. 3(a) and 3(b) where the light trajectories for two different  $R$  values, 12 and 6 mm, are presented. The

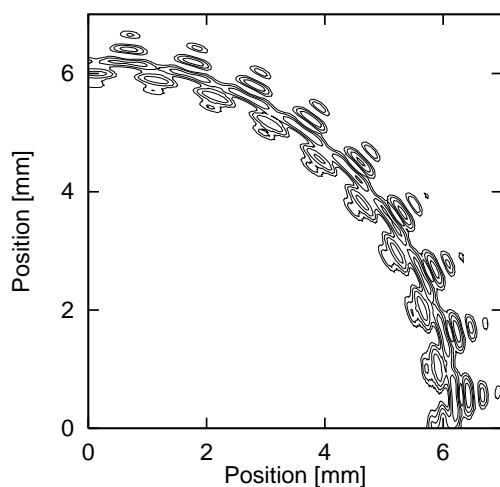


FIG. 2. Contours of equal light intensity in a curved waveguide array with  $R = 6 \text{ mm}$  and an input beam FWHM =  $10 \mu\text{m}$  ( $X$  plane). The transverse size of the contours is magnified by a factor of 70.

spatial period of the OBO in these figures is found to be 2.06 and 1.03 mm, respectively, consistent with Eq. (8). A more detailed comparison of the intensity distributions in Figs. 3(a) and 3(b) shows that the transverse localization length of the OBO is consistent with Eq. (7), in particular, its linear dependence on  $R$ .

The contours in Fig. 3(b) exhibit small radiation losses on the right-hand side of the array where the transformed refractive index is greatest; the magnitude of these losses amounts to less than 1% per OBO period for these parameters. Recall that, without the periodicity, the light would travel freely towards the region of highest transformed index on the right. The Bragg reflection associated with the periodic array restricts this free propagation, and thus reduces the radiation losses, however, it does not completely eliminate them. The residual losses are due to the optical equivalent of Landau-Zener tunneling from solid state physics. The tunneling can be reduced by increasing the radius  $R$  [see Fig. 3(a)].

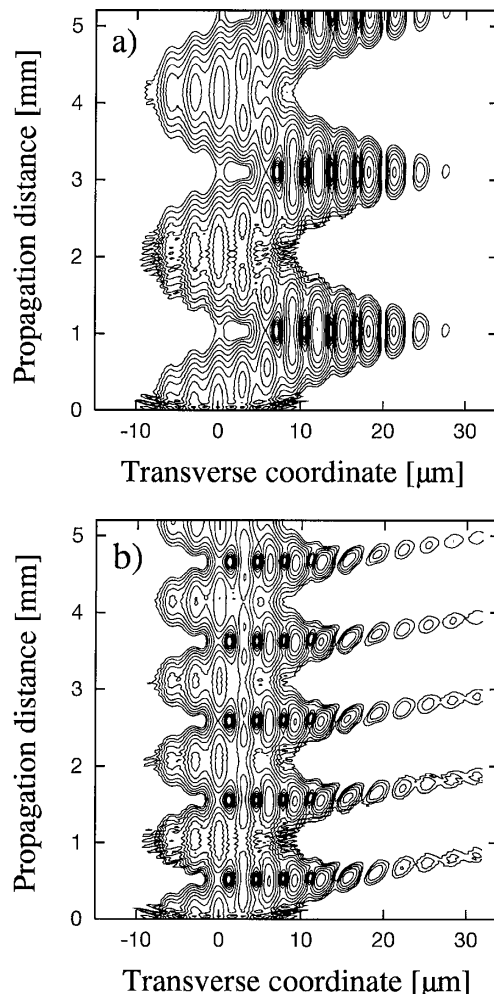


FIG. 3. Contours of equal light intensity associated with OBO ( $W$  plane). The radius of curvature is (a)  $R = 12 \text{ mm}$  and (b)  $R = 6 \text{ mm}$ , and the input beam FWHM =  $15 \mu\text{m}$ .

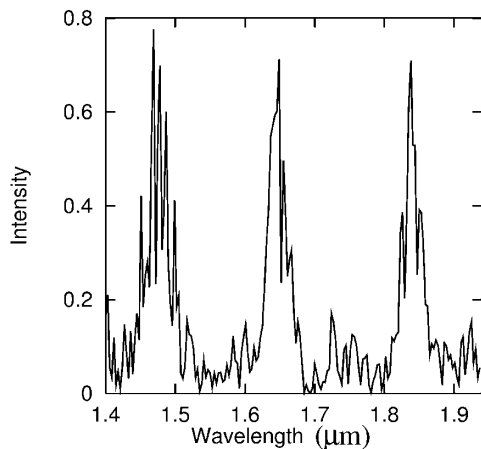


FIG. 4. Calculated transmission spectrum of the central waveguide. The propagation distance is chosen to be large ( $z_0 = 10$  mm which corresponds to  $10l$  at  $\lambda = 1.5 \mu\text{m}$  and  $R = 6$  mm), and the input beam FWHM =  $5 \mu\text{m}$ . The intensity values are normalized to the input intensity.

The fact that the intensity distributions in Figs. 2 and 3 are periodic indicates that WSL modes are equally spaced [5]. Thus, there is a ladder of the photonic orbits which are displaced by the period  $d$ . Our geometry thus shares this key characteristic with the electronic WSL.

To explore the wavelength dependence of OBO, we calculate the transmission spectrum of the central guide, i.e., the light intensity emerging from this guide as a function of wavelength. We observe a sequence of peaks in  $I(\lambda)$  dependence (see Fig. 4) which are due to OBO. In the frequency domain, the peaks are equally spaced. The spacing between them,  $\Delta f$ , is calculated from the condition that the ratio  $z_0/l$  must be an integer. Using Eq. (8), we obtain

$$\Delta f = \frac{cR}{dn_{\text{eff}} z_0}. \quad (9)$$

The strong wavelength dependence of the transmission spectrum, as shown in Fig. 4, has possible applications as a wavelength filter.

The numbers used in the simulations are appropriate for silicon optical bench technology, i.e., integrated silica waveguides on silicon substrate. This technology routinely produces high-quality, low-loss, and very complex photonic circuits. Fabricating the proposed structures is relatively simple with this technology. A tunable laser can be used to excite the array and the output intensity can be observed with a camera. By monitoring the small radiation losses shown in Fig. 3(b), one can confirm the existence of OBO directly. By varying the wavelength, the OBO properties can be further probed, and the validity of Eq. (8) can be assessed. Also, using recent innovations in the silicon optical bench technology, one may integrate optical gain and optically nonlinear materials, which may

allow the exploration of new physical properties of BO, which have no analog in the electronic case.

In conclusion, we have proposed to use curved optical waveguides for observation of optical Bloch oscillations. The refractive index distribution in this system is equivalent to the sum of a periodic term resulting from the equal spacing of the waveguides and a linear ramp, created by the curvature. We have demonstrated numerically that the light propagation in this geometry exhibits spatial Bloch oscillations with the longitudinal period depending on the radius of the curvature and the wavelength. The wavelength dependence is a unique feature of OBO which has no analogy in the solid state case.

I. T. is grateful to M. Raizen for discussions. This work was supported by the Australian Research Council.

- 
- [1] F. Bloch, *Z. Phys.* **52**, 555 (1928).
  - [2] G.H. Wannier, *Elements of Solid State Theory* (Cambridge University Press, Cambridge, England, 1959), pp. 190–193.
  - [3] E.E. Mendez, F. Agullo-Rueda, and J.M. Hong, *Phys. Rev. Lett.* **60**, 2426 (1988).
  - [4] M. Dignam and J.E. Sipe, *Phys. Rev. Lett.* **64**, 1797 (1990).
  - [5] G. Bastard, J.A. Brum, and R. Ferreira, in *Solid State Physics*, edited by H. Ehrenreich and D. Turnbull (Academic, Boston, 1991), Vol. 44.
  - [6] J. Feldmann, K. Leo, J. Shah, D.A.B. Miller, J.E. Cunningham, T. Meier, G. von Plessen, A. Schulze, P. Thomas, and S. Schmitt-Rink, *Phys. Rev. B* **46**, R7252 (1992).
  - [7] C. Waschke, H. Roskos, R. Schwedler, K. Leo, H. Kurz, and K. Köhler, *Phys. Rev. Lett.* **70**, 3319 (1993).
  - [8] Q. Niu, X.-G. Zhao, G.A. Georgakis, and M.G. Raizen, *Phys. Rev. Lett.* **76**, 4504 (1996).
  - [9] M. Ben Dahan, E. Peik, J. Reichel, Y. Castin, and C. Salomon, *Phys. Rev. Lett.* **76**, 4508 (1996).
  - [10] S.R. Wilkinson, C.F. Bharucha, K.W. Madison, Q. Niu, and M.G. Raizen, *Phys. Rev. Lett.* **76**, 4512 (1996).
  - [11] C.M. de Sterke, J.N. Bright, P.A. Krug, and T.E. Hammon, *Phys. Rev. E* **57**, 2365 (1998).
  - [12] G. Monsivais, M. del Castillo-Mussot, and F. Claro, *Phys. Rev. Lett.* **64**, 1433 (1990).
  - [13] C.M. de Sterke, J.E. Sipe, and L.A. Weller-Brophy, *Opt. Lett.* **16**, 1141 (1991).
  - [14] U. Peschel, T. Pertsch, and F. Lederer, *Opt. Lett.* **23**, 1701 (1998).
  - [15] H.G. Roskos, M.C. Nuss, J. Shah, K. Leo, D.A.B. Miller, A.M. Fox, S. Schmitt-Rink, and K. Köhler, *Phys. Rev. Lett.* **68**, 2216 (1992).
  - [16] M. Heiblum and J.H. Harris, *IEEE J. Quantum Electron.* **11**, 75 (1975).
  - [17] D. Marcuse, *Theory of Dielectric Optical Waveguides* (Academic, San Diego, 1991), 2nd ed., Chap. 8.